Modelling and Validation of the Axial Strain Distribution in WS$_2$ Flakes at WS$_2$/Epoxy/PMMA Nanocomposite under Axial Load

Tatyana Petrova[1], Elisaveta Kirilova[2], Rayka Vladova[3],
Boyan Boyadjiev[4], Wilfried Becker[5], Petia Dineva-Vladikova[6]

[1]Institute of Chemical Engineering, Bulgarian Academy of Sciences, Akad. G. Bonchev Str., bl.103, 1113 Sofia, Bulgaria (t.petrova@iche.bas.bg) ORCID 0000-0001-9073-4291; [2]Institute of Chemical Engineering, Bulgarian Academy of Sciences, Akad. G. Bonchev Str., bl.103, 1113 Sofia, Bulgaria (e.kirilova@iche.bas.bg) ORCID 0000-0002-9984-5067; [3]Institute of Chemical Engineering, Bulgarian Academy of Sciences, Akad. G. Bonchev Str., bl.103, 1113 Sofia, Bulgaria (r.vladova@iche.bas.bg) ORCID 0000-0001-7605-9904; [4]Institute of Chemical Engineering, Bulgarian Academy of Sciences, Akad. G. Bonchev Str., bl.103, 1113 Sofia, Bulgaria (boyan.boyadjiev@iche.bas.bg); [5]Institute of Structural Mechanics, TU Darmstadt, Franziska-Braun-Str. 7, L5|01 347a, 64287 Darmstadt, Germany, (becker@fsm.tu-darmstadt.de) ORCID 0000-0002-1804-236X; [6]Institute of Mechanics, Bulgarian Academy of Sciences, Acad. G. Bonchev Str., Bl.4, 1113 Sofia, Bulgaria (petia@imbm.bas.bg) ORCID 0000-0002-0994-7175

Abstract

In the present study, a two-dimensional stress-function method is applied to model the axial strain distribution in the tungsten disulfide (WS$_2$) flake embedded in an epoxy/polymethyl methacrylate nanocomposite structure subjected to an axial tension load. The analytical model strain distribution along the flake is calculated and compared with experimental and shear-lag model literature data for monolayer flake at an external strain of 0.35% and 0.55%, as well as with results for few-layer flakes at an external strain of 0.55%. The comparison shows good agreement and confirms the applicability of our model method for describing strains in nanocomposite layered structures in the elastic region of applied loads. The presented method is not appropriate for few layers flake at an external strain of 0.55% because of the appearance of relaxation zone and the formation of wrinkles in the flake.

Author Keywords. Two-dimensional Stress-function Method. Axial Strain. WS$_2$/SU-8/PMMA Nanocomposite. Applied Mechanical Load. Analytical Solutions.

Type: Research Article

1. Introduction

In recent years, two-dimensional (2D) nanomaterials such as graphene, hexagonal boron nitride (hBN), and metal dichalcogenides (MX2) have attracted a lot of attention due to their valuable properties and wide application in electronics, optoelectronics, catalysts, energy storage facilities, sensors, solar cells, lithium batteries, composites, etc. (Tan et al. 2017). The transition metal dichalcogenides (TMDs) have the general chemical formula of MX2, where X is the element of S, Se, or Te and M is the element in groups 4–10. The research interest in the graphene properties has been increased continuously since 2004, but as was reported by Mohanty, Mishra, and Khatei (2020), the graphene has a zero band gap, and it's difficult to manipulate its electronic properties for a wide variety of its applications. Therefore, researchers have explored other forms of 2D materials similar to graphene as graphyne, borophene, silicene, Si$_2$BN, stanene, plumbene, phosphorene, antimonene, and bismuthene.

The representatives of the family of TMDs are molybdenum disulfide (MoS_2), tungsten disulfide (WS_2), molybdenum diselenide ($MoSe_2$), tungsten diselenide (WSe_2), and molybdenum ditelluride ($MoTe_2$). Among the more than 40 varieties of TMDs, WS_2 and WSe_2 have attracted significant scientific attention due to their giant spin–orbit splitting, a property of particular interest for spintronics, as well as optical materials.

Most studies on the TMDs, especially for WS_2, are experimental ones, with emphasis on their electrical, optical, and mechanical properties. The modeling of the nanocomposites behaviour under external loading, which consist of 2D nanomaterials like graphene, WS_2, MoS_2, $MoSe_2$, etc., is a challenge, so far only taken up by the finite element method (FEM), using powerful and expensive commercial software packages such as ANSYS, Abaqus, COSMOS, etc. (Dai and Mishnaevsky 2014; Guo et al. 2019). At the same time, the analytical methods and models describing the behavior of a layered 2D nanocomposite under loading are few. The leading models are one-dimensional (e.g., shear-lag, non-linear shear-lag) and have been used mainly for modeling of double-layer nanocomposites containing graphene (Gong et al. 2010; Bronsgeest et al. 2015; Wang et al. 2020). There are also known two-dimensional analytical solutions (continuum mechanics, plate theory) at mechanical and/or temperature loading in layered composite structures (single lap-joint, double lap-joint) (Zhao et al. 2014), but still are not known such incorporating 2D nanoadditives or layers.

Over the last years, only some research related to modelling, predicting, and controlling the stress transfer and/or strain mapping in WS_2/polymer nanocomposites has been found in the literature (Zhang et al. 2016; Wang 2017; Deng, Sumant, and Berry 2018; Wang et al. 2020; Tang et al. 2021; Falin et al. 2021). In Zhang et al. (2016) a finite element (FE) model of a WS_2/PDMS sample under tensile strain has been represented as a strain relaxation with wrinkle formation observed on the monolayer WS_2 triangular crystals at high tensile strain. Tang et al. (2021) have proposed a more complex study on multiscale simulation, including density functional theory (DFT), molecular dynamic (MD) analysis, and FE analysis in order to analyze the WS_2 mechanical properties as a part of stress sensor and then fabricate and investigate the device for benchmarking. It has been found that the proposed FE model in this work can be used for further optimization of the device. Falin et al. (2021) have conducted an experimental study and theoretical calculations based on the FEM and DFT for the description of the elastic and strength behaviour of WS_2. In Wang (2017) and Wang et al. (2020) a combined photoluminescence (PL) spectroscopy and Raman spectroscopy have been used for an experimental description of the strain and stress transfer in exfoliated WS_2 under uniaxial strain. It has been demonstrated that the WS_2 can act as reinforcing phase in its nanocomposites and its behaviour can be predicted with shear- lag theory.

Our previous experience in this field (Kirilova et al. 2019; Petrova et al. 2022) has provided two analytical model solutions for the stress transfer in the graphene-adhesive-polymer nanocomposites, based on the two-dimensional stress-function method and minimization of complementary strain energy functional to the nanostructure. Briefly, the procedure of the solution derivation follows these three steps: First, using one unknown stress-potential function (the axial stress in graphene), the constitutive equations and boundary and contact conditions, all stresses in the structure's layers are expressed as functions of this potential and its derivatives. Then, the local and total complementary strain energies for all structure's layers are calculated, based on the integration of a functional of all stresses and strains in the layers. And finally, after the minimization of this functional, the general analytical solution of the resulted ordinary differential equation (ODE) of 4th order in respect to the potential

function after the minimization is searched for. The details are given in our previous works mentioned.

According to this method application, different analytical solutions of governing fourth-order ODE with constant coefficients for the 2D axial stress in the first layer of the nanocomposite structure (graphene), could be developed. It was ascertained, that these solutions differ mathematically, which is due to the difference in the thicknesses of the adhesive and polymer layers of the considered structures; the thickness of the graphene layer does not change.

Now, in this work, the abovementioned method was used for modelling of strains (especially axial strain in WS₂ flake) in a three-layer WS₂/SU-8/PMMA nanocomposite, subjected to a static extension load. Using two different analytical 2D solutions for axial stress, corresponding to different geometry combinations for the layer's thicknesses, the 2D model strain distributions in tungsten disulfide flake could be obtained, based on the constitutive equations of mechanics. Up to the authors' knowledge, so far only 1D analytical shear-lag model was applied to predict the axial strain in tungsten disulfide flake for WS₂-polymer structures. Validation of the obtained model solutions for axial strain in WS₂ flake was performed by comparison with experimental data and shear-lag model results from (Wang 2017) for a monolayer flake WS₂ at an external strain of 0.35% and 0.55%, and also with experimental data and shear-lag for few layer flakes WS₂ at external strain of 0.55%. The comparison confirms the applicability of the two-dimensional stress-function method for describing strains in nanocomposite layered structures in the elastic region of applied loads. For 0.55% external strain, as the applied method as well as the shear-lag are unable to describe the deformations in the middle of the experimental axial strain profile, because of the appearance of the relaxation zone in the flake and the formation of wrinkles (Zhang et al. 2016).

2. Problem statement and obtained analytical solutions for axial strain in WS₂ flake

In Figure 1 a representative volume element (RVE) of a three-layer WS₂/SU-8/PMMA nanocomposite structure is shown. The axial tensile force P (N.m) is applied to the PMMA layer, where the external load is expressed such as $\sigma_0 = P/h_2$. The coordinate system *Oxy* is placed at the left end of the structure with a length l, the y-coordinates for the layers are: $b = h_2$, $c = h_2 + h_a$, $y_t = h_2 + h_a + h_1$. Based on our previous experience, the two-dimensional stress-function method, combined with minimization of complementary strain energy functional in the nanostructure, has been applied to the structure in Figure 1. As a result, two different analytical solutions (noted here as Equation (1) and Equation (2)) for the axial stress $\sigma_{xx}^{(1)} = \sigma_1(x) = \sigma_1$ in the first layer WS₂ could be obtained. For brevity, in this study, only the final forms of the solutions are given. The details of their derivation, boundary and contact conditions and etc., could be seen in our previous works (Kirilova et al. 2019; Petrova et al. 2022).

$$\sigma_1 = C_1 \exp(\lambda_1 x) + C_2 \exp(\lambda_2 x) + C_3 \exp(\lambda_3 x) + C_4 \exp(\lambda_4 x) - A \tag{1}$$

$$\sigma_1 = \exp(-\alpha x)(M_1 \cos(\beta x) + M_2 \sin(\beta x)) + \exp(\alpha x)(M_3 \cos(\beta x) + M_4 \sin(\beta x)) - A \tag{2}$$
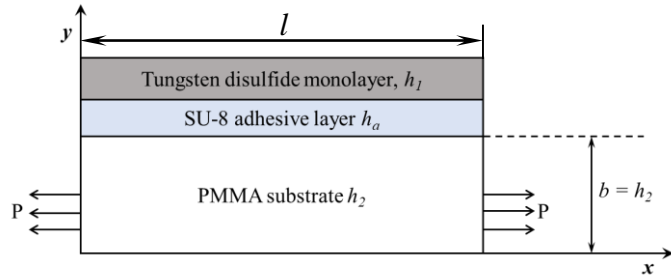
Figure 1: RVE of three-layer WS₂/SU-8/PMMA nanocomposite structure

The constants C_i and M_i are the integration constants in the model solutions, determined from the respective boundary conditions. The first solution for axial stress - Equation (1), is obtained (Petrova et al. 2022) on the base of 4 real roots $\lambda_{1,2,3,4}$ of the characteristic equation, corresponding to the 4th ODE with constant coefficients D_i - Equation (3), in respect to the axial stress σ_1. The coefficients D_i depend on the layers thicknesses and their material properties as Young's moduli and Poisson's ratios, and also on the magnitude of the applied static tensile load σ_0.

$$2D_2\sigma_1^{IV} + (2D_3 - 2D_4)\sigma_1'' + 2D_1\sigma_1 + D_5 = 0 \tag{3}$$

The second solution for the axial stress – Equation (2), has been derived on the base of 4 complex conjugate roots $\pm(\alpha \pm i\beta)$ of the same characteristic equation of the same ODE (Kirilova et al. 2019). The solutions – Equation (1) and Equation (2) have been obtained at a different sign of discriminant of the quadratic equation, corresponding to the abovementioned characteristic one; it can be positive or negative, so its roots can be real, complex or mixed. The sign of this discriminant depends on the values of the coefficients D_i of the homogeneous ODE Equation (3). The constant A in Equation (1) and Equation (2) is set as $A = D_5/2D_1$, which is a partial solution of Equation (3).

All two-dimensional stresses – axial $\sigma_{xx}^{(i)}$, shear $\sigma_{xy}^{(i)}$, and normal $\sigma_{yy}^{(i)}$ in each layer $(i = 1, a, 2)$ of the considered nanocomposite structure could be expressed in terms of the axial stress σ_1 of the WS₂ layer, and its first and second derivatives. Here only equations for the first layer will be used, namely:

$$\sigma_{xx}^{(1)} = \sigma_1(x) = \sigma_1, \qquad \sigma_{yy}^{(1)} = \frac{1}{2}(y - y_t)^2\sigma_1'', \qquad \sigma_{xy}^{(1)} = (y_t - y)\sigma_1' \tag{4}$$

Finally, using the Equations (1)÷(2) and Equation (4), the 2D strains in the first layer WS₂ of the considered nanostructure could be calculated by the following relations, based on the constitutive equations of mechanics:

$$\varepsilon_{xx}^{(1)} = \frac{\sigma_{xx}^{(1)}}{E^{(1)}} - \frac{v^{(1)}\sigma_{yy}^{(1)}}{E^{(1)}} = \frac{\sigma_1}{E^{(1)}} - \frac{v^{(1)}\sigma_{yy}^{(1)}}{E^{(1)}}, \text{if using Eq.(1) for } \sigma_1 \tag{5a}$$

$$\varepsilon_{xx}^{(1)} = \frac{\sigma_{xx}^{(1)}}{E^{(1)}} - \frac{v^{(1)}\sigma_{yy}^{(1)}}{E^{(1)}} = \frac{\sigma_1}{E^{(1)}} - \frac{v^{(1)}\sigma_{yy}^{(1)}}{E^{(1)}}, \text{if using Eq.(2) for } \sigma_1 \tag{5b}$$

where $E^{(1)}$ and $v^{(1)}$ are the Young's modulus and the Poisson's ratio of the WS₂ flake.

In the next section, a validation of the obtained model solutions (5a) and (5b) for the axial strain in the WS₂ layer was performed, based on a comparison with the experimental data and shear-lag model results taken from Wang (2017) for strain distribution in WS₂ monolayer at external strain of 0.35% and 0.55%, applied to WS₂/SU-8/PMMA nanocomposite. Our results

have been compared also with experimental data and shear-lag results (Wang 2017) for axial strain distribution in few layer WS₂ flakes with longer length in the same nanocomposite at external strain of 0.55%, to illustrate the limitation of using our model solutions for the deformations.

3. Comparison of obtained model strains with results of Wang (2017) – model validation and constrains

To validate the abovementioned model strain solutions in WS₂ layer – Equation (5a) and Equation (5b), different model layers' geometries for the studied nanocomposite WS₂-polymer structure have to be considered. The comparison will be made between these two solutions and the results for WS₂ strain distribution in the work of Wang (2017) - experimentally measured and shear-lag predicted in WS₂/SU-8/PMMA nanocomposite, subjected to the axial external loads at 0.35% and 0.55%. Wang (2017) has reported experimental and shear-lag model results for the strain distribution in monolayer WS₂ flake at 0.35% and 0.55% external loads. He has presented also experimental and shear-lag model results for WS₂ strain distribution, which corresponds to a different thickness (few layer flakes) and length of the WS₂ layer, at 0.55% external strain. Practically, for the purpose of our comparison, six different model structures, with different geometry and external loading, should be considered (Table 1). For each of the two model strain solutions (Equation (5a) and Equation (5b)) in the case of monolayer flake two different loadings 0.35% and 0.55% should be applied; in the case of few layer flake and different length an external loading of 0.55% is applied.

The values of applied external load σ_0 for monolayer at 0.35% and 0.55% external strain as in Wang (2017) are about 1.3 and 2 GPa respectively. For few layer flakes and 0.55% external strain, the corresponding σ_0 is 2.7 GPa. For the model stress and strain calculation and figures preparation, Mathcad Prime v.6.0 and Sigma Plot, v.13.0 have been used.

Geometry and properties for model structure and solution		Layer 1, Tungsten disulphide	Layer "a", Adhesive SU - 8	Layer 2, PMMA
Monolayer WS₂/SU-8/PMMA , $l = 7 \times 10^{-6}$ m				
Equation (5a) Thickness of the layer, (m)	h_i	0.65×10^{-9}	1×10^{-8}	1×10^{-6}
Equation (5b) Thickness of the layer, (m)	h_i	0.65×10^{-9}	2×10^{-8}	3×10^{-6}
Young's modulus, (Pa)	$E^{(i)}$	270×10^{9}	2×10^{9}	3.5×10^{9}
Poisson's ratio, -	$v^{(i)}$	0.22	0.22	0.35
Few layers WS₂/SU-8/PMMA, $l = 17 \times 10^{-6}$ m				
Equation (5a) Thickness of the layer, (m)	h_i	5.6×10^{-9}	1×10^{-8}	1×10^{-6}
Equation (5b) Thickness of the layer, (m)	h_i	5.6×10^{-9}	2×10^{-8}	3×10^{-6}
Young's modulus, (Pa)	$E^{(i)}$	270×10^{9}	2×10^{9}	3.5×10^{9}
Poisson's ratio, -	$v^{(i)}$	0.22	0.22	0.35

Table 1: Geometry and mechanical properties of layers' materials used in the model solutions Equation (5a) and Equation (5b) for calculation of the axial strain in the WS₂ layer, at external strain of 0.35% and 0.55%

In Figure 2, Figure 3 and Figure 4, the obtained model solutions for the axial strain in WS₂ flake(s) according to the conditions in Table 1, Equations (5a), (5b) and Equations (1), (2) and

(4), are compared with both experimental data and shear-lag method, used in the thesis of Wang (2017).

As it can be seen from Figure 2 and Figure 3, our results fit well with both the experimental data and the shear-lag predictions of Wang (2017), especially in the plateau region of the strain distribution (about 90% of flake length) and for 0.35% external strain. Equation (5b) gives a visually better description of strain distribution than Equation (5a). It could be explained with the fact that Equation (5b) gives the solution for the strain in hyperbolic sines and cosines as the shear-lag model does. On the other hand, the solution Equation (5a) consists of trigonometric sines and cosines.
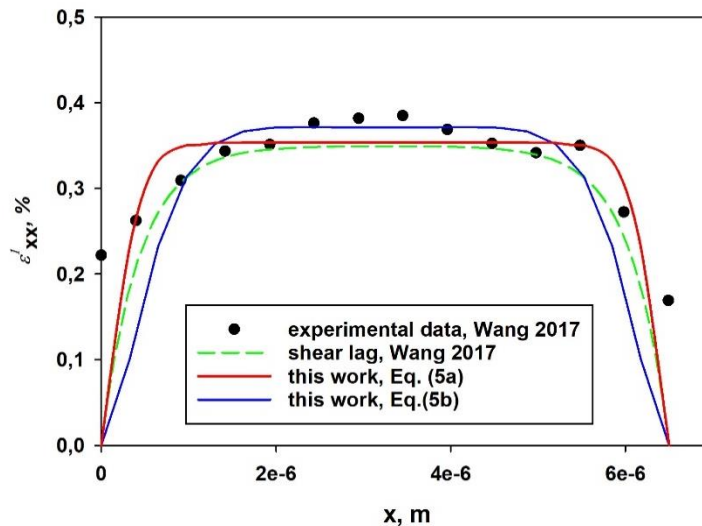

Figure 2: Comparison between the obtained model strain solutions (5a) and (5b) and both shear-lag prediction and the experimental data of Wang (2017) for strain in monolayer flake WS$_2$, at external strain of 0.35%
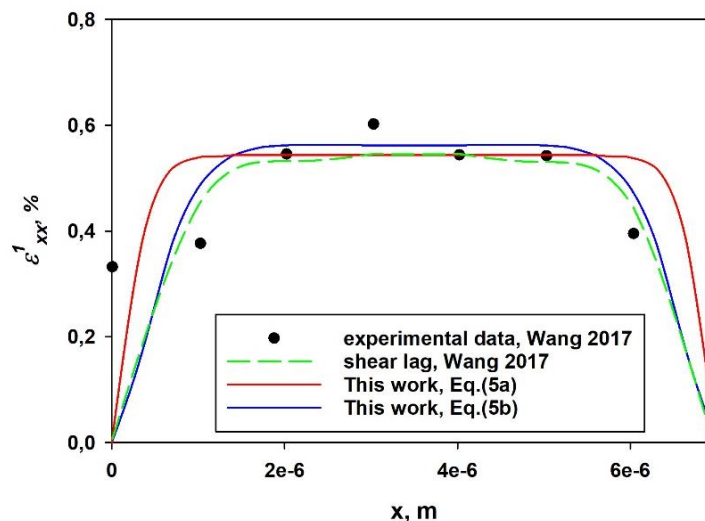

Figure 3: Comparison between the obtained model strain solutions and both shear lag prediction and experimental data of Wang (2017), for the strain in monolayer flake WS$_2$, at external strain of 0.55%

This difference is seen especially at the ends of the plateau region – for (5b) the strain curve is smoother and the plateau itself is shorter than the respective curve for (5a). The similar trend was observed for stress distribution (which will be valid for strains too) in our latest previous works for graphene/SU-8/PET (Kirilova et al. 2019) and graphene/SU-8/PMMA

(Petrova et al. 2022), where the two solutions for axial stress in first layer Equations (2) and (1) were derived, respectively. Solution (1) predicts sharper 2D stress surfaces in contrast to smoother ones for solution (2), due to the different layers' thicknesses.

It is worth mentioning, that for the purposes of considered comparison here the materials' properties and the layer's thicknesses for the adhesive and polymer layers are not of great importance, because the experimental measurements of the strain have been performed in the WS$_2$ layer only. Also, shear-lag results are 1D and do not account for 2D changes. On the other hand, recently it was experimentally observed (Jang et al. 2020), that geometry of the supported layers is important - thicker layers of PMMA gave the higher stretchability to graphene/PMMA nanocomposite structures and stability to the higher values of the external strain.

For Figure 2 and Figure 3, the respective mean relative errors between the three models – Equation (5a), Equation (5b), shear lag (Wang 2017) and experimental data, are calculated and presented in Table 2. It should be noted, that the deviation of the experimental data at the ends of the flake from the model predictions (ours and shear-lag) is visible in both figures. Shear-lag and proposed model solutions suggest, that at the ends of the flake the strain should be 0, while from experimental data distribution the opposite follows.

To Figure 2, strains in WS$_2$ at 0.35%				
Mean relative error, %	Experimental, Wang (2017)	Equation (5a), this work	Equation (5b), this work	Shear-lag, Wang (2017)
Experimental, Wang (2017)	—			
Equation (5a), this work	13.92	—		
Equation (5b), this work	19.32	22.16	—	
Shear-lag, Wang (2017)	19.27	19.48	9.29	—

To Figure 3, strains in WS$_2$ at 0.55%				
Mean relative error, %	Experimental, Wang (2017)	Equation (5a), this work	Equation (5b), this work	Shear-lag, Wang (2017)
Experimental, Wang (2017)	—			
Equation (5a), this work	16.05	—		
Equation (5b), this work	17.65	25.02	—	
Shear-lag, Wang (2017)	34.24	19.37	20.46	—

Table 2: Mean relative errors (%) between experimental data (Wang 2017), Equation (5a), Equation (5b) and Shear-lag (Wang 2017), for WS$_2$ strain distributions in Figures 2 and 3

From Figure 4 it can be seen that neither shear-lag, nor our results are able to describe the experimental "triangle" profile of the strain in the middle, for few layer flakes, at external strain of 0.55%. In the work of Wang et al. (2020) a similar statement as ours is reported at 0.55% external strain and few layer flakes - "*the strain drops sharply in the middle of the flake although the strain distribution of other parts still approximately follows the shear lag curve*". These authors (Wang et al. 2020) have explained this with the experimentally observed formation of cracks in the flake, perpendicular to the tensile axis. In Zhang et al. (2016) after performed experimental and FEM simulations it was concluded, that may be this effect is due to the appearance of a relaxation zone in the flake and the formation of wrinkles. Such kind of effects in the strain distribution out of the elastic region of the applied strains is also observed for graphene flakes in the thesis of Gong (2012).

Despite the huge deviation in the middle region of the flake for external strain 0.55 %, our Equation (5a) and shear-lag fits well to the rest of the experimental data profile in Figure 4.

Outside the elastic region, these "triangle" strain distributions observed in 2D nanomaterials like graphene, MoS₂, WS₂ etc., could be modeled using numerical (FEM) cohesive models (Liu et al. 2014) or by recently reported multiscale simulation (Tang et al. 2021).
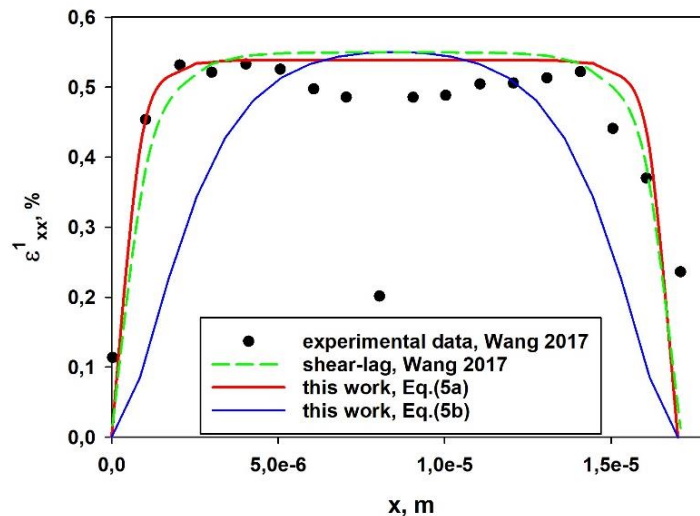

Figure 4: Comparison between the obtained model solutions for axial strain in WS₂ and both shear lag prediction and experimental data of Wang (2017) for the strain in few layer flakes WS₂, at external strain of 0.55%

4. Conclusions

In this work, the 2D stress function method combined with minimization of complementary strain energy functional was used for the first time for modelling of tungsten disulfide axial strain in a three-layer WS₂/SU-8/PMMA nanocomposite, subjected to a static extension load. Validation of the obtained model solutions for axial strain in WS₂ flake was performed by comparison with experimental data and shear-lag model results from Wang (2017) for a monolayer flake at an external strain of 0.35 % and 0.55 %, and also with experimental data and shear-lag for few layer flakes at external strain of 0.55 %. The comparison shows good agreement and confirms the applicability of the two-dimensional stress-function method for describing strains in nanocomposite layered structures in the elastic region of the applied loads. The limitation of the model application outside the elastic region is due to the appearance of defects in the 2D flake like wrinkles and cracks.

References

Bronsgeest, M. S., N. Bendiab, S. Mathur, A. Kimouche, H. T. Johnson, J. Coraux, and P. Pochet. 2015. "Strain relaxation in CVD graphene: Wrinkling with shear lag". *Nano Letters* 15, no. 8: 5098-104. https://doi.org/10.1021/acs.nanolett.5b01246.

Dai, G., and L. Mishnaevsky. 2014. "Graphene reinforced nanocomposites: 3D simulation of damage and fracture". *Computational Materials Science* 95: 684-92. https://doi.org/10.1016/j.commatsci.2014.08.011.

Deng, S., A. V. Sumant, and V. Berry. 2018. "Strain engineering in two-dimensional nanomaterials beyond graphene". *Nano Today* 22: 14-35. https://doi.org/10.1016/j.nantod.2018.07.001.

Falin, A., M. Holwill, H. Lv, W. Gan, J. Cheng, R. Zhang, D. Qian, M. R. Barnett, E. J. G. Santos, K. S. Novoselov, et al. 2021. "Mechanical properties of atomically thin tungsten

dichalcogenides: WS$_2$, WSe$_2$, and WTe$_2$". *ACS Nano* 15, no. 2: 2600-10. https://doi.org/10.1021/acsnano.0c07430.

Gong, L., I. A. Kinloch, R. J. Young, I. Riaz, R. Jalil, and K. S. Novoselov. 2010. "Interfacial stress transfer in a graphene monolayer nanocomposite". *Advanced Materials* 22, no. 24: 2694-97. https://doi.org/10.1002/adma.200904264.

Gong, L. 2012. "Deformation micromechanics of graphene nanocomposites". PhD diss., School of Materials, Faculty of Engineering and Physical Sciences, The University of Manchester, Manchester, UK.

Guo, Z., L. Song, G. B. Chai, Z. Li, Y. Li, and Z. Wang. 2019. "Multiscale finite element analyses on mechanical properties of graphene-reinforced composites". *Mechanics of Advanced Materials and Structures* 26, no. 20: 1735-42. https://doi.org/10.1080/15376494.2018.1447176.

Jang, H., Z. Dai, K. H. Ha, S. K. Ameri, and N. Lu. 2020. "Stretchability of PMMA-supported CVD graphene and of its electrical contacts". *2D Materials* 7, no. 1: Article number 014003. https://doi.org/10.1088/2053-1583/ab4c0f.

Kirilova, E., T. Petrova, W. Becker, and J. Ivanova. 2019. "Mathematical modelling of stresses in graphene polymer nanocomposites under static extension load". In *2019 IEEE 14th Nanotechnology Materials and Devices Conference, NMDC 2019*, 1-4. IEEE. https://doi.org/10.1109/NMDC47361.2019.9084003.

Liu, Z., M. Amani, S. Najmaei, Q. Xu, X. Zou, W. Zhou, T. Yu, C. Qiu, A. G. Birdwell, F. J. Crowne, et al. 2014. "Strain and structure heterogeneity in MoS 2 atomic layers grown by chemical vapour deposition". *Nature Communications* 5: Article number 5246. https://doi.org/10.1038/ncomms6246.

Mohanty, R., A. Mishra, and J. Khatei. 2020. "Two-dimensional nanostructures for advanced applications". In *ACS Symposium Series*, 1-31. https://doi.org/10.1021/bk-2020-1353.ch001.

Petrova, T., E. Kirilova, W. Becker, and J. Ivanova. 2022. "Two-dimensional stress and strain analysis for graphenepolymer nanocomposite under axial load". *Journal of Applied and Computational Mechanics* 8, no. 3: 1065-75. https://doi.org/10.22055/jacm.2022.38834.3292.

Tan, C., X. Cao, X. J. Wu, Q. He, J. Yang, X. Zhang, J. Chen, W. Zhao, S. Han, G. H. Nam, et al. 2017. "Recent advances in ultrathin two-dimensional nanomaterials". *Chemical Reviews* 117, no. 9: 6225-331. https://doi.org/10.1021/acs.chemrev.6b00558.

Tang, H., D. Hu, Z. Cui, H. Ye, and G. Zhang. 2021. "Effects of defect and temperature on the mechanical performance of WS$_2$: A multiscale analysis". *Journal of Physical Chemistry C* 125, no. 4: 2680-90. https://doi.org/10.1021/acs.jpcc.0c09897.

Wang, F. 2017. "Raman and photoluminescence spectroscopic studies of the micromechanics of WS$_2$ nanocomposites". PhD diss., The University of Manchester, Manchester, UK.

Wang, F., S. Li, M. A. Bissett, I. A. Kinloch, Z. Li, and R. J. Young. 2020. "Strain engineering in monolayer WS$_2$and WS$_2$nanocomposites". *2D Materials* 7, no. 4: Article number 045022. https://doi.org/10.1088/2053-1583/ababf1.

Zhang, Q., Z. Chang, G. Xu, Z. Wang, Y. Zhang, Z. Q. Xu, S. Chen, Q. Bao, J. Z. Liu, Y. W. Mai, et al. 2016. "Strain relaxation of monolayer WS$_2$ on plastic substrate". *Advanced Functional Materials* 26, no. 47: 8707-14. https://doi.org/10.1002/adfm.201603064.

Zhao, B., Z. H. Lu, and Y. N. Lu. 2014. "Two-dimensional analytical solution of elastic stresses for balanced single-lap joints - Variational method". *International Journal of Adhesion and Adhesives* 49: 115-26. https://doi.org/10.1016/j.ijadhadh.2013.12.026.

Acknowledgments